

# Field-Incidence Noise Transmission Loss of General Aviation Aircraft Double-Wall Configurations

Ferdinand W. Grosveld\*

*The Bionetics Corporation, Hampton, Virginia*

Theoretical formulations have been developed to describe the transmission of reverberant sound through an infinite, semi-infinite, and a finite double-panel structure. The model incorporates the fundamental resonance frequency of each of the panels, the mass-air-mass resonances of the structure, the standing-wave-resonances in the cavity between the panels, and finally the coincidence resonance region, where the exciting sound pressure wave and flexural waves of each of the panels coincide. It is shown that phase cancellation effects of pressure waves reflected from the cavity boundaries back into the cavity allows the transmission loss of a finite double-panel structure to be approximated by a finite double panel mounted in an infinite baffle having no cavity boundaries. Comparison of the theory with high-quality transmission loss data yields good agreement in the mass-controlled frequency region. It is shown that the application of acoustic blankets to the double-panel structure does not eliminate the mass-air-mass resonances if those occur at low frequencies. It is concluded that this frequency region of low-noise transmission loss is a potential interior-noise problem area for propeller-driven aircraft having a double-panel fuselage construction.

## Nomenclature

$a, b$	= linear panel dimensions
$c$	= speed of sound in air
$d$	= panel spacing
$E$	= Young's modulus
$E_r$	= complex ray representation defined in Eq. (20)
$f$	= frequency
$f_0$	= mass-air-mass resonance for normal angle of incidence
$f_\theta$	= mass-air-mass resonance for angle of incidence $\theta$
$i$	= integer (1,2)
$I$	= number of components used to average the term in Eq. (27)
INT	= integer part of an expression
$j$	= $\sqrt{-1}$
$k$	= wave number
$k_{\max}$	= number of frequencies summed in each one-third octave band
$L$	= panel length
$m$	= band number
$m_i$	= mass per unit area of $i$ th panel
$n$	= number of reflections
$N$	= number of incidence bands
$P$	= total transmitted sound
$q_i$	= quantity for $i$ th panel defined in Eq. (7)
$r$	= number of reflections off the cavity boundaries
$R$	= quantity defined in Eq. (17)
$S$	= panel area
$t$	= panel thickness
TL	= noise transmission loss of a single panel
TL <sub>1/3</sub>	= one-third octave band double-panel transmission loss
TL <sub>inf</sub>	= transmission loss of infinite double panel
TL <sub>si</sub>	= transmission loss of semi-infinite double panel
$x$	= $x_1 x_2$
$x_i$	= fraction of incident sound on $i$ th panel defined in Eq. (1)
$y$	= defined in Eq. (3)
$\alpha$	= $jk \sin \theta$

$\beta$	= $jk b \sin \theta$
$\eta$	= loss factor
$\theta$	= angle of sound incidence
$\theta_l$	= limiting angle of sound incidence
$\nu$	= Poisson's ratio
$\rho$	= mass density
$\tau$	= transmission coefficient
$\bar{\tau}$	= field-incidence transmission coefficient
$\phi$	= angle defined in Eq. (8)
$\psi$	= $N\phi$
$\omega$	= angular frequency
$\omega_r$	= angular fundamental panel resonance frequency

## Introduction

THE fuselage sidewalls of almost all general aviation aircraft are designed as multiple-wall configurations consisting of skin, insulating material, damping material, impervious septa, and trim panel. High levels of interior noise are found in these light aircraft due to engine and propeller noise that is transmitted through the sidewall fuselage. A multiple-layered sidewall offers acoustical benefits in the higher frequency regions,<sup>1-15</sup> but at lower frequencies resonances are introduced as the masses of the individual panels interact with the medium between them acting as a spring. Standing waves in the cavity between the panels cause additional resonances. Previously, researchers have identified these mass-air-mass and standing-wave resonances but no theoretical formulation is available that is valid at all frequencies including the fundamental and coincidence frequencies and is verified by experimental data. The purpose of this paper is to develop a theoretical formulation for the problem of noise transmission loss through a double-wall structure and to compare this theory with high-quality transmission loss data obtained in the NASA Langley Transmission Loss Apparatus. The importance of mass-air-mass resonances for propeller-driven general aviation aircraft will be demonstrated. Transmission loss data of double panels with acoustic blankets in between will be presented.

## Double-Panel Noise Transmission Loss

Beranek and Work<sup>2</sup> and London<sup>3</sup> have presented theoretical models that describe the transmission loss of infinite double panels. Beranek and Work's theory is derived

Received March 5, 1984; revision received Sept. 28, 1984. Copyright © American Institute of Aeronautics and Astronautics, Inc., 1984. All rights reserved.

\*Aero-Space Research Engineer. Member AIAA.

by using the principle of the continuity of acoustic impedance at the interfaces of the various media. London approaches the problem by applying boundary conditions at the panel surface when it is subjected to a progressive harmonic plane wave at oblique angle of incidence. Boundary conditions include continuity of wave potential and equality of the pressure wave particle velocity with the panel displacement velocity. These theories generate results identical to those discussed by Mulholland et al.<sup>8</sup> The authors introduce a multiple-reflection theory to predict the transmission loss of a double panel by modeling a plane progressive wave as bands of individual rays which are obliquely incident on the structure. The rays are tracked along their path, applying single-panel transmission loss theory each time they impinge on one of the panels. The theory in its simplest form, when integrated over all random incidence angles, produces the same results as obtained in Refs. 2 and 3. Agreement between these theories for infinite double panels and transmission loss measurements on finite structures is poor. As the theoretical corrective measures in Refs. 3 and 9 are not substantiated by experimental data, the theory for sound transmission through double-panel structures will be investigated in an attempt to predict actual transmission loss more accurately. The analysis will be based on multiple-reflection theory as initiated in Ref. 8, and will be applied to the three double-panel models shown in Fig. 1.

#### Infinite Panel

The sound transmission problem is first considered for a plane wave of unit pressure amplitude and angular frequency  $\omega$  incident upon the infinite panel at an angle  $\theta$ . Considering a small area at an arbitrary location on the surface, the incident pressure wave can be modeled as a ray. When the ray impinges on the panel a fraction  $x_1$  is transmitted while the remainder  $(1-x_1)$  is reflected back. The fraction  $x_1$  is determined by the single-panel transmission loss and is given by

$$x_1 = \sqrt{\tau_1(\omega, \theta)} \quad (1)$$

where the transmission coefficient  $\tau(\omega, \theta)$  is defined by<sup>16,17</sup>:

$$\tau(\omega, \theta) = \left\{ \left[ 1 + \eta \left( \frac{\omega m}{2\rho c} \cos\theta \right) \left( \frac{\omega^2 E t^3 \sin^4\theta}{12(1-\nu^2)mc^4} \right) \right] + \left[ \left( \frac{\omega m}{2\rho c} \cos\theta \right) \left( 1 - \frac{\omega^2 E t^3 \sin^4\theta}{12(1-\nu^2)mc^4} \right) \right]^2 \right\}^{-1} \quad (2)$$

The ray travels across the airspace between the two panels and meets the second panel causing a fraction  $x_1 x_2$  of the original unit pressure amplitude to emerge. The reflected wave travels back and meets the first panel where part of it is again reflected and part of it emerges from the second panel with an amplitude that is reduced to  $x_1 x_2 (1-x_1)(1-x_2)$ . The phase

difference between the successively emerging waves is given as  $-2jkd/\cos\theta$ , which is representative of the distance traveled. This procedure will continue indefinitely and is illustrated in Fig. 2. The traveling wave is assumed to be harmonic in time ( $\exp j\omega t$ ) but this factor, being common to all terms, is not written explicitly. Figure 3 shows the total contribution of all rays that emerge at an arbitrary point on the second panel. The first ray contributes  $x_1 x_2$ . A second ray will add  $x_1 x_2 (1-x_1)(1-x_2) \exp(-2jkd/\cos\theta)$  but will be out of phase with the first ray of the plane wave by an additional  $2jkd \tan\theta \sin\theta$ , which results in  $x_1 x_2 (1-x_1)(1-x_2) \exp(-2jkd \cos\theta)$ . The third ray will contribute  $x_1 x_2 (1-x_1)^2 (1-x_2)^2 \exp(-4jkd \cos\theta)$  and likewise for all succeeding rays. Thus, the total of all emerging rays can be given by

$$\sum_{n=1}^{\infty} xy^{n-1} = \frac{x}{1-y} \quad (3)$$

where  $y = (1-x_1)(1-x_2) \exp(-2jkd \cos\theta)$  and  $x = x_1 x_2$ . As this will be invariable for any location on the second panel, the transmission loss for an infinite panel is defined by

$$TL_{inf} = 10 \log \{ |1-y|/x \}^2 \quad (4)$$

This result is the same as in Refs. 2, 3, and 8. The present study differs from the method employed by Mulholland et al.<sup>8</sup> in that the total contribution of the sound rays is considered at one point rather than the total sound transmitted by one ray. The results of these two methods are identical for an infinite panel because all rays, at a given angle of sound incidence, have a constant phase relationship when they emerge from the second panel. Using the equations  $x_1 = 1/(1+jq_1)$

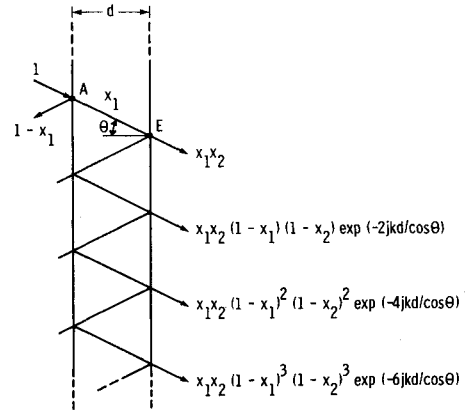


Fig. 2 Double-panel sound transmission for a ray of unit pressure amplitude incident at angle  $\theta$ .

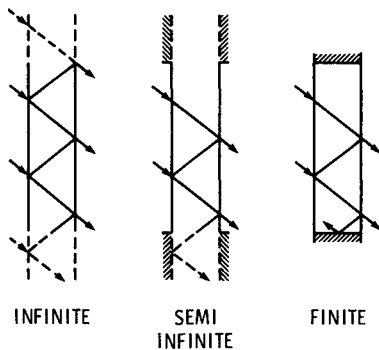


Fig. 1 Infinite, semi-infinite, and finite double-panel models.

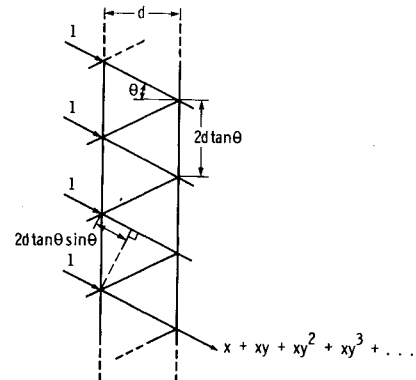


Fig. 3 Transmitted sound at one location on the second panel for a plane wave of unit pressure amplitude incident at angle  $\theta$ .

and  $x_2 = 1/(1+jq_2)$  the real and imaginary parts of the transmission loss given by Eq. (4) can be separated

$$TL_{inf} = 10 \log \left[ \left| \{ 1 + q_1 q_2 (\cos \phi - 1) + j(q_1 + q_2 - q_1 q_2 \sin \phi) \} \right|^2 \right] \quad (5)$$

and the resulting transmission loss of an infinite double panel at oblique sound incidence is given by

$$TL_{inf} = 10 \log \left[ 1 + (q_1^2 + q_2^2) - 2q_1 q_2 \{-q_1 q_2 + (q_1 q_2 - 1) \cos \phi - (q_1 + q_2) \sin \phi\} \right] \quad (6)$$

where

$$q_i = \frac{m_i \omega^2 \cos \theta}{2 \omega \rho c} \left\{ 1 - \frac{\omega^2 E (1+j\eta) t^3 \sin^4 \theta}{12 (1-\nu^2) c^4 m_i} \right\} \quad (7)$$

and

$$\phi = 2k d \cos \theta \quad (8)$$

In a reverberant sound field uncorrelated waves from many directions are incident on the structure. The field-incidence transmission coefficient is found by averaging over all of the components in the field

$$\bar{\tau}(\omega) = \int_0^{\theta_0} \tau(\omega, \theta) \cos \theta \sin \theta d\theta / \int_0^{\theta_0} \cos \theta \sin \theta d\theta \quad (9)$$

and is related to the field-incidence transmission loss by

$$TL(\omega) = 10 \log [1/\bar{\tau}(\omega)] \quad (10)$$

Mass-air-mass resonances will occur at frequencies where the total mass reactance of the panels equals the stiffness reactance of the airspace and can be found by setting the transmission loss in Eq. (6) to zero

$$f_\theta(\theta) = \frac{1}{2\pi \cos \theta} \left\{ \frac{\rho c^2 (m_1 + m_2)}{m_1 m_2 d} \right\}^{1/2} \quad (11)$$

This frequency region is bounded by

$$f_0 \leq f_\theta \leq f_{\theta_0} \quad (12)$$

In this frequency region there will be some angle of sound incidence for which the sound attenuation of the double panel is zero. However, after integration over all angles of field incidence, the total transmission loss of the double panel will always be greater than zero.

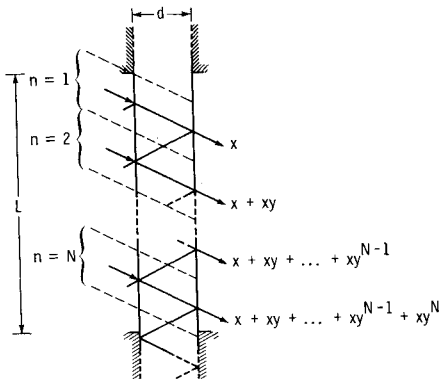


Fig. 4 Semi-infinite double-panel model.

### Semi-Infinite Double Panel

In a more restricted case, two square panels with finite dimensions are mounted onto an infinite baffle. This is referred to as a semi-infinite double panel. In this model, illustrated in Fig. 4, the incident waves are split up into  $N$  bands, where  $N$  may be found from

$$N = \text{INT} \left\{ \frac{L - d \tan \theta}{2d \tan \theta} \right\} \quad (13)$$

The first incident band produces a band of emerging rays each of which is given by  $x$ . The second band of emerging rays consists of contribution  $x$  from the second incident band and a contribution  $xy$  from the first. The third band of emerging waves is the sum of the contributions of the first three incident bands and is given by  $x + xy + xy^2$ . The  $N$ th band of emerging waves is thus the sum of the contributions of all  $(N-1)$  bands. Summing all of the rays emerging from the second panel yields

$$\sum_{n=1}^N (N-n+1)xy^{n-1} = \frac{x}{(1-y)^2} \{N(1-y) - y(1-y^N)\} \quad (14)$$

Each emerging ray in the  $n$ th band will be identical in amplitude and phase to others in that band. The transmission loss, in complex form, then follows from

$$TL_{si} = 10 \log \left\{ \left| \frac{(N+0.5)(1-y)^2}{x\{N(1-y) - y(1-y^N)\}} \right|^2 \right\} \quad (15)$$

Separating the real and imaginary parts in Eq. (15), taking the modulus, and squaring the expression yields the transmission loss for a semi-infinite double panel at angle of sound in-

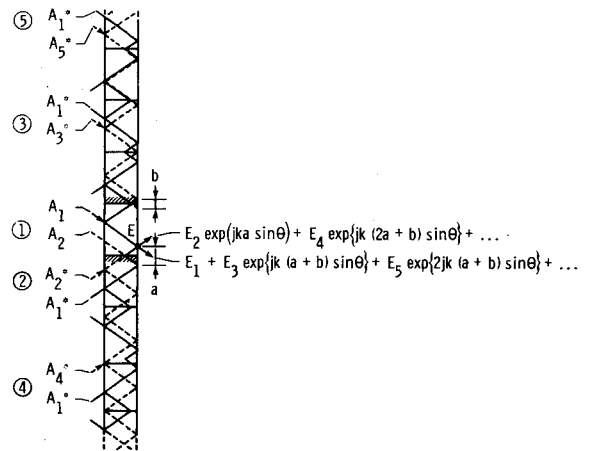


Fig. 5 Mirror image model of finite double panel.

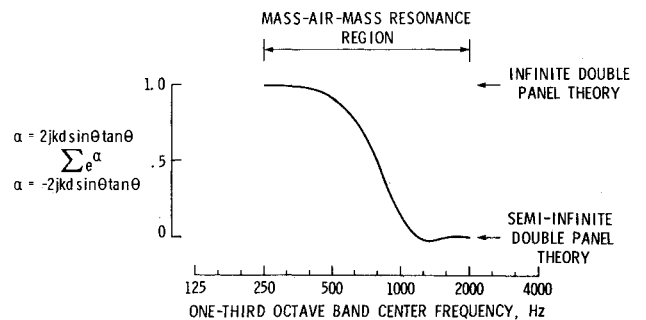


Fig. 6 Phase relationship term  $e^\alpha$  as a function of mass-air-mass resonance frequency.

cidence  $\theta$

$$\begin{aligned} TL_{si} = 10 \log \left\{ \left[ (N+0.5)^2 (1-2R \cos \Psi + R^2)^2 (1+q_1^2) (1+q_2^2) \right] \right. \\ \left. + [N - (1+N)R \cos \Psi + R^{N+1} \cos(N+1)\Psi]^2 \right. \\ \left. + \{ (N-1)R \sin \Psi + R^{N+1} \sin(N+1)\Psi \}^2 \right\} \quad (16) \end{aligned}$$

where

$$R = \frac{q_1 q_2}{[(1+q_1^2)(1+q_2^2)]^{1/2}} \quad (17)$$

and where  $q_i$  may include the fundamental resonance frequency and its damping. To obtain the field-incidence transmission loss Eq. (16) is integrated over all angles of field incidence in the same manner as described for the infinite double panel.

#### Finite Double Panel

The finite double-panel model differs from the semi-infinite case in that the rays, upon reaching the cavity boundaries, are reflected back into the cavity to produce an additional series of emerging rays. This process, illustrated in Figs. 1 and 5, shows that the second series of rays emerge after being reflected from the lower cavity boundary. If  $N$  bands are considered, the total contribution of this second series is given by

$$E_2 = \sum_{m=0}^{N-1} \sum_{n=m+2}^{N+m+1} x y^{n-1} \quad (18)$$

where  $m$  is the band number and  $n$  the number of reflections which occur between the time the ray is incident and the time it emerges. The rays then continue and will be reflected off the other cavity boundary to produce a third series of emerging rays given by

$$E_3 = \sum_{m=N}^{2N-1} \sum_{n=m+2}^{N+m+1} x y^{n-1} \quad (19)$$

The  $r$ th series can be represented by

$$E_r = \sum_{m=(r-2)N}^{(r-1)N-1} \sum_{n=m+2}^{N+m+1} x y^{n-1} \quad (20)$$

where the quantities  $x$  and  $y$  are the same as for the infinite and semi-infinite double panels. Equation (20) can be evaluated to give

$$E_r = \frac{x(1-y^N)^2 y^{(r-2)N+1}}{(1-y)^2} \quad (21)$$

which is the summation of all emerging rays after  $(r-1)$  reflections off the cavity boundaries by  $N$  incident rays. To obtain the correct boundary conditions at the second panel surface, the contribution of all emerging rays at each location on that panel has to be evaluated. The first series of emerging waves is described by the semi-infinite case. To aid in the identification of the reflected rays which contribute at a particular location on the second panel, a mirror image sequence is shown in Fig. 5. For reasons of simplicity, only one ray ( $A_1$ ) is incident on the double panel in region 1 and only one ray ( $E_1$ ) is emerging. The rays in region 2 are the

mirror images of the rays in region 1, the rays in region 4 are the mirror images of those in region 2, and so on, thus creating an infinite chain of mirror images. At the location  $E$  on the second panel, where  $E_1$  is emerging, a number of other rays will contribute to the total sound transmission. After the incident ray with amplitude  $A_2$  is reflected at the lower cavity boundary of the finite double panel it will emerge as a ray with amplitude  $E_2$  on the second panel. The mirror image of  $A_2$  is indicated in Fig. 5 and can easily be found by extending the line from the emerging point into region 2 (dashed line). This ray will be out of phase with the ray  $A_1$  by a factor of  $\exp j k a \sin \theta$ . Other reflected rays that will reach the emerging point  $E$  can be found by extending the dashed line further as depicted in Fig. 5. Rays in between regions 2 and 4 are traveling in the downward direction and will not reach point  $E$ . From region 4,  $A_4$  will contribute  $E_4$  but will be out of phase by a factor  $\exp j k (2a+b) \sin \theta$ . This concept can be extended to give an infinite series of contributions at location  $E$ .

When mirror images with respect to the upper cavity boundary are considered, similar arguments will lead to a contribution of  $E_3 \exp j k (a+b) \sin \theta$  by  $A_3$  and a ray  $E_5 \exp 2 j k (a+b) \sin \theta$  will emerge at point  $E$  due to  $A_5$ . This process will also continue indefinitely and all odd contributions can be represented by the odd components of an infinite series. All rays that can possibly emerge at location  $E$  on the second panel have now been considered. In summary, substituting Eq. (21) for  $E_r$ , all even series contribute

$$\sum_{r=1}^{\infty} \exp \{ \sin \theta j k [(a+b)r - a] \} E_{2r} = \frac{x(1-y^N)^2}{(1-y)^2} \frac{y e^{\alpha}}{1 - e^{\beta + \alpha} y^{2N}} \quad (22)$$

and all odd series provide the contribution

$$\sum_{r=1}^{\infty} \exp \{ \sin \theta j k [(a+b)r] \} E_{2r+1} = \frac{x(1-y^N)^2}{(1-y)^2} \frac{y y^N e^{\beta + \alpha}}{1 - e^{\beta + \alpha} y^{2N}} \quad (23)$$

which are traveling in a downward direction. The emerging rays in one band are no longer equal, as was the case for the infinite and semi-infinite double panels, but depend on  $a$  and  $b$ . These factors will vary between  $-2k d \tan \theta$  and  $+2k d \tan \theta$  depending on the location of the reflection at the cavity boundaries. Their sum will be constant and smaller than  $k d \tan \theta$  (Fig. 5). One may write

$$\frac{(a+b)}{2} = L - \left\{ \text{INT} \left( \frac{L}{d \tan \theta} \right) d \tan \theta \right\} \quad (24)$$

The total transmitted sound for a finite double panel, due to  $N$  incident rays of unit pressure amplitude, is determined by the summation of the expressions in Eqs. (14), (22), and (23)

$$P = \frac{x}{(1-y)^2} \left\{ N(1-y) - y(1-y^N) + y(1-y^N)^2 \frac{e^{\alpha} + e^{\beta + \alpha} y^N}{1 - e^{\beta + \alpha} y^{2N}} \right\} \quad (25)$$

It can be shown that by setting  $\alpha$  and  $\beta$  to zero, which means that all rays after being reflected from the cavity boundaries will emerge at the same location with a constant phase relationship, Eq. (25) reduces to

$$p = Nx / (1-y) \quad (26)$$

which is identical to the total transmitted sound of an infinite double panel. The result in Eq. (26) was found by Cummings and Mulholland<sup>9</sup> for the infinite double panel as well as for a

finite double panel without absorption material along the cavity boundaries. The authors obtained this result since they did not consider any phase changes in the emerging rays after reflection from the cavity boundaries.

To investigate the effect of these phase changes, the term  $e^\alpha$  in Eq. (25) is evaluated by partitioning the range over which  $\alpha$  varies into an arbitrary (large) number of components ( $I$ ). The average phase change for these components then is found by

$$\frac{1}{2I} \sum_{i=1}^I \{e^{-j\alpha_i/I} + e^{j\alpha_i/I}\} = \frac{1}{I} \sum_{i=1}^I \cos(j\alpha_i/I \times k d \tan \theta \sin \theta) \quad (27)$$

and will be dependent on frequency, panel spacing, and angle of incidence. This average phase change will be particularly important at resonances where the transmission loss is very low. In the frequency region of mass-air-mass resonances, the frequency at which a resonance occurs ( $f_\theta$ ) is related to the angle of sound incidence by

$$f_\theta = f_0 / \cos \theta \quad (28)$$

Equation (27) is evaluated for the specific case of two aluminum panels with a 0.042-m spacing and with  $f_0 = 250$  Hz, which is representative of the transmission loss measurements reported in a subsequent section of this paper. Figure 6 shows that in the resonance region  $e^\alpha$  will go to zero very rapidly when frequency increases. As  $e^{\beta+\alpha}$  in Eq. (25) will behave in a similar manner, the third term in that equation becomes negligible as frequency increases, reducing the expression to that for the total transmitted sound of a semi-infinite panel. This suggests that in the mass-air-mass resonance frequency region, transmission loss of a finite panel can be approximated by the transmission loss of an infinite panel at the lower resonance frequencies and by the transmission loss of a semi-infinite panel at the higher resonance frequencies. The average transmission loss for infinite, semi-infinite, and finite double panels is ap-

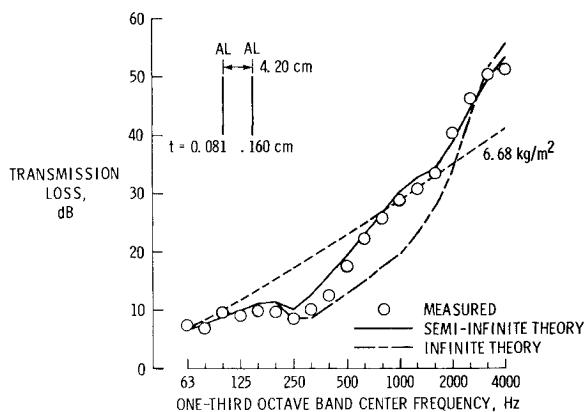


Fig. 7 Comparison of measured field-incidence transmission loss and infinite and semi-infinite double-panel theories.

proximately the same for the frequency regions in which no resonances are present.

### Experimental Data

To validate the theoretical results, transmission loss measurements were conducted in the NASA Langley Transmission Loss Apparatus which, along with the measurement methodology, is described in Ref. 18. The double-panel test program presented here included six different  $1.15 \times 1.46$ -m double-panel configurations in which the components had varying mass and stiffness properties. Panel thickness, mass per unit area, panel spacing, and calculated limiting mass-air-mass resonance frequencies are tabulated in Table 1. To insure the inclusion of the mass-air-mass resonance frequency region, the measurements are taken over a frequency range extending from the 63-Hz one-third octave band up to and including the 4000-Hz one-third octave band. The accuracy of the measurements is within 1-1.5 dB in the very-low-frequency bands (<200 Hz) and within tenths of a decibel for the higher frequency bands.<sup>18</sup>

### Comparison Between Theory and Experimental Results

In a reverberant environment a theoretically infinite number of plane waves is incident on the panel surface at all possible angles up to a limiting value  $\theta_r$ . This is referred to as field incidence of the sound. The limiting angle has been established to be 81 deg for this facility which agrees well with limiting values found by other researchers.<sup>9,16</sup> As these plane waves have random phase relationships, the average transmission loss may be found by integrating over all angles of field incidence [Eq. (9)]. The field-incidence transmission loss for the infinite and semi-infinite double-panel configurations was computed using Eqs. (6), (9), and (16) utilizing Simpson's trapezoidal rule<sup>19</sup> with a 3-deg angle-of-incidence increment. To enable comparison between theoretical predictions and experimental third-octave band data the sound pressure levels at 14 frequencies ( $k_{\max}$ ), equally divided over each third-octave band, were summed according to

$$TL_{1/3} = 10 \log \left\{ k_{\max} / \sum_{k=1}^{k_{\max}} 10^{TL/10} \right\} \quad (29)$$

All calculations were performed on a desktop computer.

In Fig. 7 the theoretical results for the infinite and semi-infinite double panels are compared with measured noise transmission loss data for a structure consisting of two 0.160-cm-thick aluminum panels having a 4.2-cm spacing. For comparison with a single panel having a mass per unit area equal to the double panel, the transmission loss according to the classical mass law has been calculated and is given by the solid, almost straight, line. The theory, as presented in this paper, suggests that in the mass-air-mass resonance frequency region the finite double-panel transmission loss can be approximated by infinite panel theory at lower resonance

Table 1 Double-panel configurations tested in the NASA Langley Research Center Transmission Loss Apparatus

Panel 1			Panel 2			Mass-air-mass resonance, Hz	
Material <sup>a</sup>	Thickness, cm	Mass/area, kg/m <sup>2</sup>	Material	Thickness, cm	Mass/area, kg/m <sup>2</sup>	Spacing, cm	Lower Upper
AL	0.081	2.25	AL	0.160	4.43	1.43	413 1986
AL	0.081	2.25	AL	0.160	4.43	4.20	244 1559
AL	0.081	2.25	MLV	0.051	4.84	2.20	407 1958
AL	0.160	4.43	MLV	0.216	4.25	2.20	276 1328
AL	0.081	2.25	PX	0.635	7.49	4.20	224 1431
AL <sup>b</sup>	N/A	4.06	PW	0.635	2.10	9.14	170 1085

<sup>a</sup> AL = aluminum, MLV = mass-loaded vinyl (two densities), PX = plexiglass, PW = plywood trimpanel. <sup>b</sup> Flat aircraft structure (skin thickness of 0.081 cm).

frequencies and by the semi-infinite panel theory at higher frequencies. The lower resonance frequencies in the measured data occur where the resonances are driven by angles of sound incidence close to normal. Since most of the sound for these small angles will emerge from the second panel before being reflected from the cavity boundaries, the effect of destructive interference between rays is minimal. It also means that the rays that reflect from the cavity boundaries are small in amplitude since they have already encountered the sound transmission process many times. Therefore, the difference between the infinite and semi-infinite panel transmission loss predictions is small in this frequency region and the semi-

infinite theory should give a reasonable prediction. A more accurate prediction of the double-wall transmission loss would be possible utilizing Eq. (25), but after separating the real and imaginary parts this equation becomes unwieldy and impractical. Therefore, the measured transmission loss data presented in subsequent figures will be compared with the semi-infinite panel theory. Figures 8-12 show that for several double-panel configurations, where the mass per unit area, panel material, and panel spacing are varied, the semi-infinite double-panel theory yields good predictions of the actual

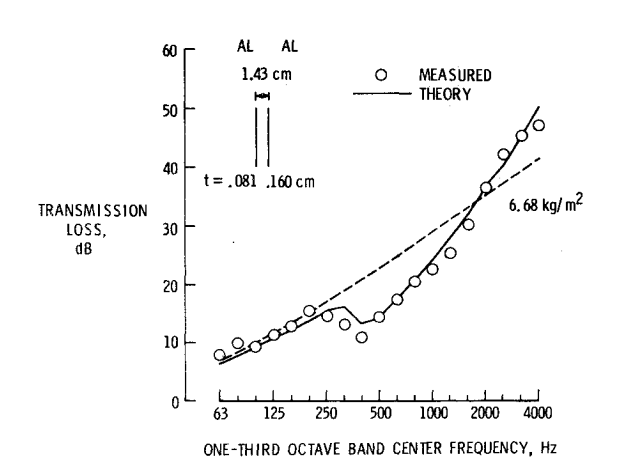


Fig. 8 Double-panel transmission loss of aluminum panels, 0.081- and 0.160-cm thick.

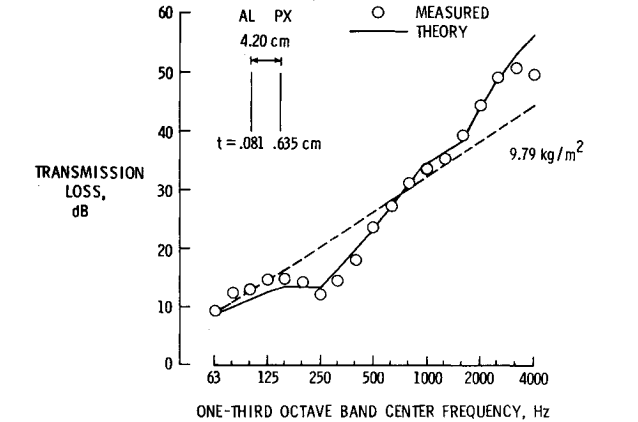


Fig. 11 Field-incidence double-panel transmission loss of a 0.635-cm plexiglass and a 0.081-cm aluminum panel.

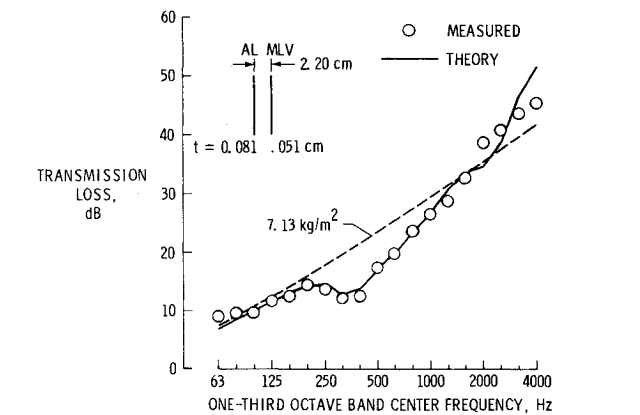


Fig. 9 Double-panel transmission loss of a 0.051-cm mass-loaded vinyl and a 0.081-cm aluminum panel.

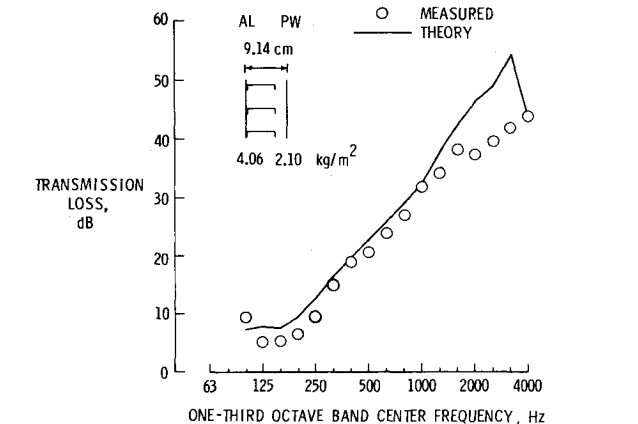


Fig. 12 Field-incidence double-panel transmission loss of a simulated aircraft fuselage sidewall.

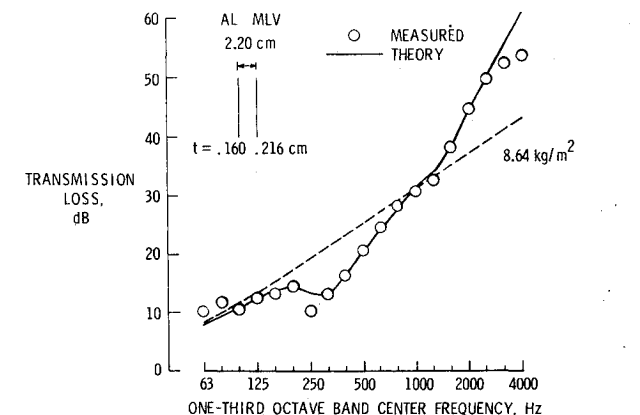


Fig. 10 Double-panel transmission loss of a 0.216-cm mass-loaded vinyl and a 0.160-cm aluminum panel.

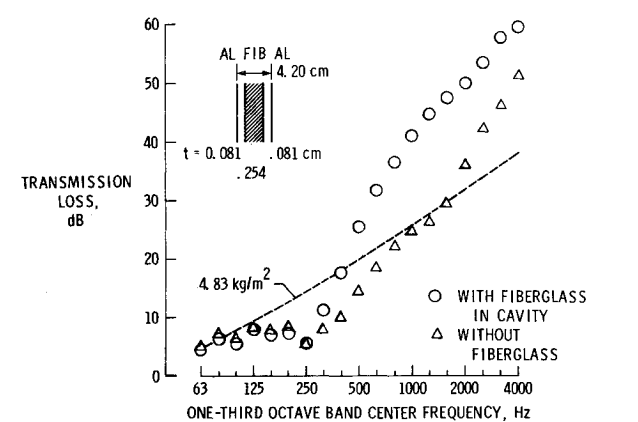


Fig. 13 Transmission loss of a double panel with and without a fiberglass blanket in the cavity.

transmission loss. The prediction is within 3 dB of the measured data over a wide range of frequencies. It should be noted that the stiffness of the panels does not play a significant role because the panels are relatively lightweight and have large dimensions ( $1.15 \times 1.46$  m). The boundary conditions of the double panel become increasingly more important as smaller panels are used.

Figure 13 shows the measured transmission loss of two 0.081-cm-thick aluminum panels with and without a fiberglass blanket in the cavity between the panels. This acoustic blanket is ineffective below the 315-Hz one-third octave band. The 2.54-cm-thick blanket does not fill the whole cavity, which has a 4.20-cm panel separation, but previous measurements have shown that even four layers of fiberglass are equally ineffective at these frequencies.<sup>20</sup> The fundamental blade passage frequency of propeller-driven aircraft generally lies between 70 and 180 Hz. If the mass-air-mass resonances coincide with the blade passage frequency or its harmonics and occur at frequencies where the fiberglass does not provide any transmission loss, an interior-noise problem might arise. No predictions for the effect of the fiberglass blanket on the noise transmission loss have been made but the method used in Refs. 20 and 21 could be implemented in the semi-infinite panel theory to give such a prediction.

### Conclusions

Transmission loss theories for infinite, semi-infinite, and finite double-panel configurations have been developed to predict the transmission loss of double-panel structures. The infinite panel theory inadequately predicts the transmission loss in the frequency region where mass-air-mass resonances occur. It has been shown that, for the finite case, destructive interference occurs as the phase relationships between emerging rays is not constant after rays are reflected from the cavity boundaries. Although the finite double-panel theory might give the most accurate predictions, the calculations are cumbersome and impractical. The semi-infinite double-panel theory yields good agreement with transmission loss measurements for a wide variety of double-panel configurations and over a broad range of frequencies. For double panels where the mass-air-mass resonances occur at low frequencies ( $<315$  Hz), the application of acoustical absorption material in the cavity between the panels is ineffective. This results in a potential interior-noise problem for propeller-driven aircraft when the highest excitation levels (at the blade passage frequency and its harmonics) coincide with the frequency region of minimum transmission loss.

### Acknowledgments

This research was supported by NASA Langley Research Center, Contract NAS1-16978, Dr. C. A. Powell, Technical Monitor.

### References

<sup>1</sup>Kimball, A. L., "Theory of Transmission of Plane Sound Waves Through Multiple Partitions," *Journal of the Acoustical Society of America*, Vol. 7, March 1936, p. 222.

<sup>2</sup>Beranek, L. L. and Work, G. A., "Sound Transmission Through Multiple Structures Containing Flexible Blankets," *Journal of the Acoustical Society of America*, Vol. 21, July 1949, p. 419.

<sup>3</sup>London, A., "Transmission of Reverberant Sound Through Double Walls," *Journal of the Acoustical Society of America*, Vol. 22, March 1950, p. 270.

<sup>4</sup>Lyon, R. H. and Maidanik, G., "Power Flow Between Linearly Coupled Oscillators," *Journal of the Acoustical Society of America*, Vol. 34, May 1962, p. 623.

<sup>5</sup>Lyon, R. H. and Eichler, E., "Random Vibration of Connected Structures," *Journal of the Acoustical Society of America*, Vol. 36, No. 7, July 1964, pp. 1344-1354.

<sup>6</sup>Lyon, R. H. and Sharton, T. D., "Vibrational-Energy Transmission in a Three-Element Structure," *Journal of the Acoustical Society of America*, Vol. 38, Aug. 1965, p. 253.

<sup>7</sup>White, R. H. and Powell, A., "Transmission of Random Sound and Vibration Through a Rectangular Double Wall," *Journal of the Acoustical Society of America*, Vol. 40, No. 4, April 1966, pp. 821-832.

<sup>8</sup>Mulholland, K. A., Parbrook, H. D., and Cummings, A., "The Transmission Loss of Double Panels," *Journal of Sound and Vibration*, Vol. 6, No. 3, March 1967, pp. 324-334.

<sup>9</sup>Cummings, A. and Mulholland, K. A., "The Transmission Loss of Finite Sized Double Panels in a Random Incidence Sound Field," *Journal of Sound and Vibration*, Vol. 8, No. 1, Jan. 1968, pp. 126-133.

<sup>10</sup>Mulholland, K. A., Price, A. J., and Parbrook, H. D., "Transmission Loss of Multiple Panels in a Random Incidence Field," *Journal of the Acoustical Society of America*, Vol. 43, No. 6, June 1968, pp. 1432-1435.

<sup>11</sup>Sharp, B. H. and Beauchamp, J. W., "The Transmission Loss of Multi-Layer Structures," *Journal of Sound and Vibration*, Vol. 9, No. 3, March 1969, pp. 383-392.

<sup>12</sup>Price, A. J. and Crocker, M. J., "Sound Transmission Through Double Panels Using Statistical Energy Analysis," *Journal of the Acoustical Society of America*, Vol. 47, No. 3, March 1970, pp. 683-693.

<sup>13</sup>Sharp, B. H., "A Study of Techniques to Increase the Sound Insulation of Building Elements," Wyle Laboratories, El Segundo, Calif., Rept. WR 73-5, June 1973.

<sup>14</sup>Grosveld, F. M. W. A., "Study of Typical Parameters that Affect Sound Transmission Through General Aviation Aircraft Structures," Doctoral Dissertation, Flight Research Laboratory, University of Kansas, Lawrence, Kan., KU-FRL-417-13, Aug. 1980.

<sup>15</sup>Grosveld, F., Navaneethan, R., and Roskam, J., "Noise Reduction Characteristics of General Aviation Type Dual Pane Windows," AIAA Paper 80-1874, Aug. 1980.

<sup>16</sup>London, A., "Transmission of Reverberant Sound Through Single Walls," *Journal of Research of the National Bureau of Standards*, Research Paper RP 1998, Vol. 42, June 1949, p. 605.

<sup>17</sup>Von Cremer, L., "Theorie der Schalldämmung Dünner Wände bei Schrägem Einfall," *Akustische Zeitschrift*, Vol. 7, May 1942, pp. 81-104 (in German).

<sup>18</sup>Grosveld, F. W., "Characteristics of the Transmission Loss Apparatus at NASA Langley Research Center," NASA CR 172153, June 1983.

<sup>19</sup>Abramowitz, M. and Stegun, I., eds., *Handbook of Mathematical Functions*, Dover Publications, New York, 1972.

<sup>20</sup>Grosveld, F. W., "Noise Transmission Through Sidewall Treatments Applicable to Twin-Engine Turboprop Aircraft," AIAA Paper 83-0695, April 1983.

<sup>21</sup>Grosveld, F. W. and Mixson, J. S., "Noise Transmission Through an Acoustically Treated and Honeycomb Stiffened Aircraft Sidewall," AIAA Paper 84-2329, Oct. 1984.